



## Research article

## Improving the solubility of nilotinib through novel spray-dried solid dispersions

Maikel Herbrink<sup>a,\*</sup>, Jan H.M. Schellens<sup>a,b</sup>, Jos H. Beijnen<sup>a,b</sup>, Bastiaan Nuijen<sup>a</sup><sup>a</sup> Department of Pharmacy and Pharmacology, The Netherlands Cancer Institute – Antoni van Leeuwenhoek Hospital and MC Slotervaart, Louwesweg 6, 1066 EC, Amsterdam, The Netherlands<sup>b</sup> Department of Pharmaceutical Sciences, Utrecht University, Universiteitsweg 99, 3584 CG Utrecht, The Netherlands

## ARTICLE INFO

## Article history:

Received 24 April 2017

Received in revised form 3 July 2017

Accepted 4 July 2017

Available online 8 July 2017

## Chemical compounds studied in this article:

Nilotinib hydrochloride (PubChem CID: 16006490)

## Keywords:

Nilotinib

Solubility

Spray drying

Dissolution

Formulation improvement

## ABSTRACT

The tyrosine kinase inhibitor nilotinib has a very low aqueous solubility and a low and variable oral bioavailability. A pharmaceutical formulation with an improved solubility may enhance the bioavailability and reduce the variability thereof and of the pharmacokinetics. The aim of this study was to enhance the solubility of nilotinib by developing a spray dried solid dispersion. A broad selection of polymer excipients were tested for solubilizing properties. The spray drying technique was used to produce solid dispersions of nilotinib hydrochloride (NH) in matrices of the best performing polymers. Both the dissolution and physicochemical characteristics of the formulations were studied using a pH-switch dissolution model and conventional microscopic, thermal and spectrometric techniques. Of the tested spray dried solid dispersions, the ones containing the co-block polymer Soluplus<sup>®</sup> performed best in terms of *in vitro* dissolution properties. Further testing led to an optimized weight ratio of 1:7 (NH: Soluplus<sup>®</sup>) that improved the solubility up to 630-fold compared to crystalline NH (1.5 µg/mL) in simulated intestinal fluid. This effect can be attributed to the amorphization of NH and the solubilization of the drug due to micelle formation. A spray dried solid dispersion formulation of NH with Soluplus<sup>®</sup> in a ratio of 1:7 was developed that showed a significant increase in solubility.

© 2017 Elsevier B.V. All rights reserved.

## 1. Introduction

The tyrosine kinase inhibitor nilotinib is registered for the treatment of newly diagnosed adults with Philadelphia chromosome positive myeloid leukemia (Ph+ CML) in the chronic phase (European Medicines Agency (EMA), 2007; US Food and Drug Administration (FDA), 2007a). It is also indicated for the treatment of chronic and accelerated phase Ph+ CML in adult patients that are resistant or intolerant to prior therapy that included imatinib. The drug is marketed as Tasigna<sup>®</sup> since it received authorization in 2007 by both the European Medicines Agency (EMA) and the US Food and Drug Administration (FDA). The recommended dose ranges between 300 and 400 mg twice daily and is administered orally (US Food and Drug Administration (FDA), 2010).

Nilotinib hydrochloride (Fig. 1) (NH) monohydrate is deemed poorly to moderately soluble (US Food and Drug Administration (FDA), 2007a). Furthermore, the permeability of nilotinib is considered to be low in part due to efflux by P-glycoprotein (Pgp)-

transporters in the gut wall (Shukla et al., 2011). The drug is thus classified in the biopharmaceutics classification system (BCS) as class IV (US Food and Drug Administration (FDA), 2007a). This indicates that its absorption and bioavailability is hindered by solubility and permeability. NH is currently formulated as physical mixture with lactose, croscopvidone and poloxamer 188 in an immediate release capsule. No study into the absolute oral bioavailability of the Tasigna<sup>®</sup> formulation has been performed hitherto. Based on mass balance studies, however, the bioavailability is estimated to be approximately 30% (European Medicines Agency (EMA), 2007). The intra- and interpatient variability in the pharmacokinetic parameters  $C_{max}$  and area under the plasma-time curve (AUC) range between 32 and 72% (European Medicines Agency (EMA), 2007; Tanaka et al., 2010). Since bioavailability and drug exposure are tightly linked,  $C_{max}$  and AUC are also influenced by poor solubility and permeability. Variation in drug exposure may cause drug plasma levels to be inadequately low or toxically high (Herbrink et al., 2015). Enhancing the solubility of NH monohydrate through improvement of its formulation may increase the bioavailability and possibly reduce pharmacokinetic variability.

Drug solubility enhancement can be achieved through the use of various techniques (Kawabata et al., 2011; Keen et al., 2013;

\* Corresponding author.

E-mail address: [m.herbrink@nki.nl](mailto:m.herbrink@nki.nl) (M. Herbrink).



a 25 mL beaker containing 10 mL of medium. Temperature was kept at 37 °C and the medium was stirred at 200 rpm. The commercial formulation (Tasigna<sup>®</sup>) and the capsulated investigational formulations were tested in a larger dissolution volume of 200 mL. Dissolution tests were performed in single pH environment (simulated intestinal fluid (SGF), pH 6.8) and a pH-switch system. In this system, the 25 mL beaker contained 10 mL of simulated gastric fluid (SGF), pH 1.6. The sample was kept in this environment for 30 min after which the pH and composition was changed into that of SIF in a step-wise manner by briefly adding phosphate or carbonate buffer. The switch of pH and the composition adjustment was typically completed within 32 min. Samples were taken at designated time points, filtrated using a 0.45 µm filter and diluted 1/1 with methanol. All samples were subsequently analysed using HPLC.

## 2.6. Micelle size measurements

The presence and size of micelles was detected and measured using a Zetasizer Nano S90 particle size analyser (Malvern Instruments, Worcestershire, UK). Samples were taken from the dissolution media, placed in polystyrene cuvettes (Malvern Instruments) and analysed in threefold at 10 analyses per measurement.

## 2.7. Electron microscopy (EM)

The morphology of the bulk and spray-dried powders were studied using Scanning Electron Microscopy (SEM). Samples were placed on conducting double sided adhesive tape and on an aluminium holder. Samples were sputter-coated with gold using a SCD 040 sputter coater (Oerlikon, Balzers, Liechtenstein). Imaging was performed through back-scattering with a Sigma Field Emission Gemini system (Zeiss, Oberkochen, Germany).

The shape and size of micelles were visualized with Transmission Electron Microscopy (TEM). Samples from dissolution media were diluted 100 times and were applied on Agar<sup>®</sup> formvar/carbon coated copper grids (van Loenen instruments, Zaandam, The Netherlands). The samples were negatively stained with 2% (w/w) phosphotungstic acid and were dried for 10 min prior to the microscopy. The micrographs were recorded using a Tecnai T12 G2 Spirit Biotwin set-up (FEI company, Hillsboro, OR, USA).

## 2.8. Fourier transform infrared spectroscopy (FT-IR)

Infrared spectra were recorded from 600 to 4000 cm<sup>-1</sup> with a resolution of 2 cm<sup>-1</sup> with a FT-IR 8400S Spectrophotometer equipped with a Golden Gate<sup>®</sup> (Shimadzu, 's-Hertogenbosch, The Netherlands). A total of 64 scans were averaged into one spectrum.

## 2.9. Modulated differential scanning calorimetry (MDSC)

MDSC measurements were performed with a discovery differential scanning calorimeter (DSC) (TA Instruments, New Castle, DE, USA). Temperature scale and heat flow were calibrated with Indium. Samples of approximately 3 mg powder were weighed into Tzero aluminium pans (TA Instruments), sealed and placed in the autosampler. Each sample was equilibrated at 20 °C for 3 min, after which the sample was heated to 225 °C at a speed of 3 °C/min with a modulated temperature amplitude of 1 °C per period of 60 s.

## 2.10. X-ray powder diffraction (XRD)

X-ray diffraction of powder samples was performed with an X'pert pro diffractometer equipped with an X-celerator

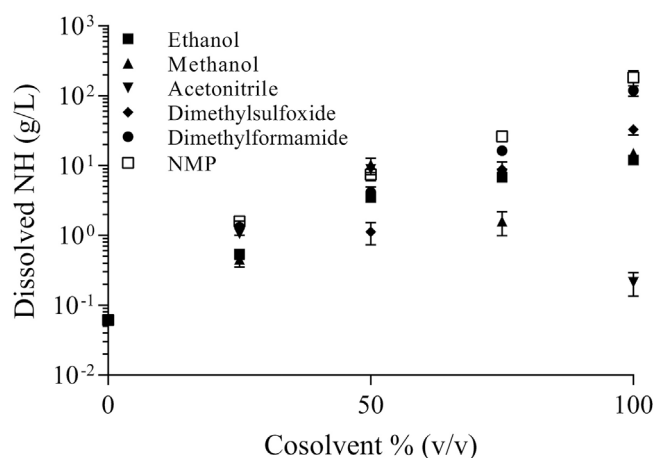


Fig. 2. Equilibrium solubility of NH in various cosolvent systems.

(PANalytical, Almelo, The Netherlands). Samples were placed in a 0.5 mm deep metal sample holder. Samples were scanned at a current of 30 mA and a tension of 40 kV. The scanning range was 10–60° 2-θ, with a step size of 0.020° 2-θ and a scanning speed of 0.002° 2-θ per second.

## 2.11. Residual solvents

Residual ethanol was determined with capillary gas chromatography (GC) analysis. Samples of approximately 50 mg of powder were dissolved or suspended in 5.0 mL water and shaken for 3 h. Aliquots were subsequently filtered and transferred to autosampler vials. Analyses were performed using 6890N GC system (Agilent, Santa Clara, CA, USA) equipped with a Flame-ionization detector (Agilent) and a RTX-1301 capillary column (3.0 µm film, 30 m × 0.53 mm; Restek Corporation, Bellefonte, PA, USA).

## 3. Results and discussion

### 3.1. Solubility and spray dry settings

In order to design an efficient spray drying protocol for NH, the solubility of the compound was assessed in various cosolvent systems. Fig. 2 presents the relationship between solubility and the cosolvent percentage. The applicability of the cosolvent systems with the highest solubility (>10 g/L) in the spray drying process was investigated. Table 1. lists the minimum required settings for the various systems. The spray drying process proved to be inefficient when carried out with the high-boiling point solvents DMSO, DMF and NMP. The process with methanol and ethanol was found to be similar in terms of spray dryer settings. Ethanol was selected because it is the least toxic of the two solvents. The spray drying process was further optimized for ethanol so that residual ethanol was below 100 ppm. Bulk and spray-dried Soluplus<sup>®</sup> were compared (dissolution, FTIR and micelle size) and no significant differences were found that would indicate changed physicochemical properties. The spray-dried formulations were analysed by HPLC to investigate possible degradation of NH during spray drying or due to interaction with Soluplus<sup>®</sup>. No evidence of this was observed in any of the spray-dried compositions.

### 3.2. Dissolution behaviour and formulation selection

The dissolution profile of the marketed formulation Tasigna<sup>®</sup> was investigated. Fig. 3A presents the dissolution curves (n = 3) of both the Tasigna<sup>®</sup> capsule and its decapsulated powder. The first

**Table 1**  
Spray dryer settings during applicability investigation of various cosolvent systems.

Solvent system	Inlet temperature (°C)	Outlet temperature (°C)	Limiting factor
75% DMF	155	140	Residual solvent present $T_{out} < 140^{\circ}\text{C}$ : Deposition of solvent $T_{out} > 130^{\circ}\text{C}$ : Polymer residue in drying column outlet
75% NMP	160	145	Residual solvent present
Ethanol	95	55	None
Methanol	90	50	Relatively toxic
DMSO/ DMF/ NMP	>160	>140	$T_{out} < 150^{\circ}\text{C}$ : Deposition of solvent $T_{out} > 130^{\circ}\text{C}$ : Polymer residue in drying column outlet Required low feed flow rate

30 min of the curve represent the stomach (pH 1.6) in which the percentage of dissolved NH adds up to approximately 26%. At time points 35, 40 and 45 min a relatively small decrease to 23% in dissolved drug is seen when the pH increases from 1.6 to 3.2. From 50 min on the dissolved amount decreases to less than 1% when the pH is elevated above 5.2 and is subsequently adjusted to 6.8. This behaviour agrees with the pH-solubility curve (Fig. 3B) and the observations by Jesson et al. (Jesson et al., 2014). The solubility of NH at higher pH values can be considered its bottleneck. Therefore, improving the drug's solubility at pH 6.8 was taken as a starting point in this study.

Fig. 4 shows the results from the excipient screening experiments after both 2 and 24 h. This manner of solubility testing is based on the worst-case-scenario where crystalline drug is solubilized by an excipient at a pH in which it is very poorly soluble. NH monohydrate has a solubility of approximately 1.5  $\mu\text{g}/\text{mL}$  in this buffer system. The tests show that Kollidon VA64, 12PF, Soluplus<sup>®</sup> and Lutrol F68 display the highest maintaining increase in solubility. For this reason, these excipients were selected for further formulation development. The increase in solubility may be due to non-complexing hydrophilic and/or hydrophobic interaction between the excipients and the drug (Bansal et al., 2007; Li et al., 2012).

The increase in solubility by Soluplus<sup>®</sup> between 2 and 24 h is possibly the result of the relative high viscosity of the solution, in comparison to the other solutions. This slows the process of wetting and dissolution to continue after the initial 2 h.

With the above four excipients both PM and SD formulations with different ratios between drug and excipient were produced.

Table 2 lists these formulations. The dissolution behaviour of the formulations was tested using the pH-switch system. The results are presented in Fig. 5. Fig. 5A shows the dissolution curves of crystalline and amorphous NH. Both forms have very different solubilities at stomach pH (38% against 83%) but show a very similar decrease in solubility when the pH is increased towards 6.8. The amorphous drug structure has an increased initial stomach solubility but still needs a 'parachute' in the intestinal medium to prevent recrystallization. The PMs (Fig. 5B–E) all exhibited similar dissolution properties as the crystalline drug in SGF, the resulting polymer concentrations in the dissolution medium of the tested PMs are likely too low to aid the dissolution and increase the solubility of NH in SGF. The desired 'parachute' effect was only observed with the Soluplus<sup>®</sup> formulations.

The dissolution curves of the SD formulations show an increased solubility in SGF, indicating the enhanced apparent solubility of the amorphous drug with 100% (1 mg/mL) solubility for both Soluplus<sup>®</sup> and Kollidon VA64. During the transition from pH 1.2 to 6.8, Lutrol F68 and Kollidon 12PF were unable to maintain an increased solubility in both compositions. Soluplus<sup>®</sup> SD 1/5 and 1/10 and Kollidon VA64 1/10 did offer a 'parachute' effect of which Soluplus<sup>®</sup> 1/10 showed the best performance. Based on these results, Soluplus<sup>®</sup> was chosen for further formulation development.

SDs with 5 different NH/Soluplus<sup>®</sup> compositions were prepared and subjected to dissolution experiments to further investigate the influence of Soluplus<sup>®</sup> on the solubility of NH. The results are presented in Fig. 6A. Fig. 6B shows the percentage dissolved NH as a function of the Soluplus<sup>®</sup> equivalent parts. From this apparent relationship, it can be concluded that a higher number of equivalent parts of Soluplus<sup>®</sup> within pharmaceutical relevant volumes would not further increase the solubility of NH at pH 6.8. The composition 1/7 was selected as the best performing formulation as it offers the highest solubility at pH 6.8 with the lowest total formulation volume. The 1/7 composition may make for a bulky dosage form when the same dose of NH is needed. An *in vivo* study should point out whether the formulation increases the bioavailability of NH. In that case, less of the formulation is required to reach adequate drug plasma levels and administration of large amounts are not needed.

### 3.3. Micelle size measurements

As Fig. 6A demonstrates, the solubility of NH permanently sharply collapses for formulation S during the pH increase. The other formulations all show a decrease in solubility during the switch that is related to the Soluplus<sup>®</sup> equivalent parts, after which the solubility increases to a seemingly constant level. The drop in solubility coincided with the solutions turning opaque.

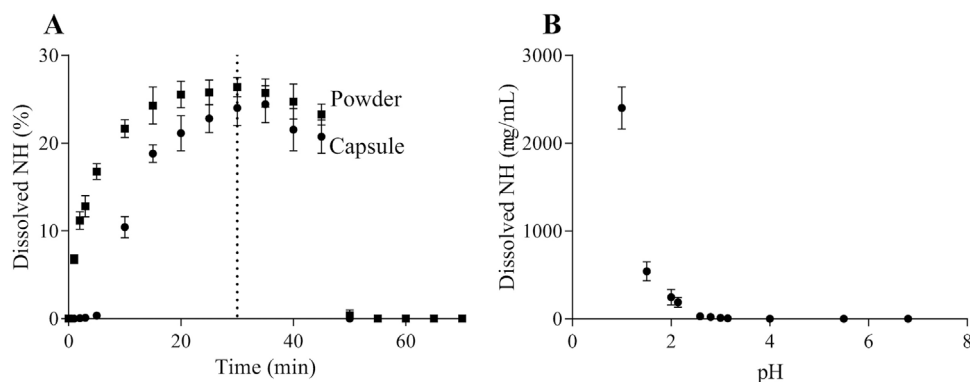


**Fig. 3.** A. Dissolution curves of Tasigna<sup>®</sup> capsules and decapsulated Tasigna<sup>®</sup> powder; B. pH-solubility curve of NH. The dotted line indicates the start of the pH-switch.

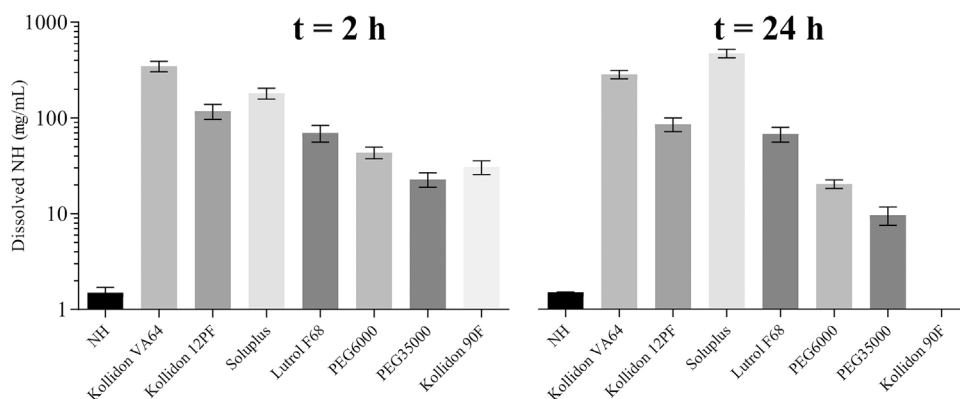


Fig. 4. Excipient screening results: NH solubility after 2 and 24 h.

At different time points during the dissolution of formulations S to W, samples were taken to measure the micelle diameters of which Fig. 7A and B presents the results. The observed opacity during the solubility drop can be linked to the sudden increase of the micelle diameter. The large micelles (>450 nm) are filtered out and the incorporated nilotinib within these micelles is subsequently not quantified by HPLC. This clarifies the apparent 'drop' in solubility.

To test whether the phenomenon is not related to the dissolution medium, a pH-switch system was designed that leads to a SIF<sub>sp</sub> with a carbonate buffer. The same pattern was observed as with the phosphate system although the micelle diameters in the carbonate system were generally larger. This distinction is important, since the intestinal medium *in vivo* is a carbonate buffered system instead of a phosphate buffered one. Despite this difference in size, the micelle for formulations U,V and W regained a size of <100 nm at pH > 6. Fig. 7A and B also presents the size of Soluplus<sup>®</sup> micelles without NH where the pH-dependent increase does not occur. An explanation for the behaviour of the NH/Soluplus<sup>®</sup> micelles might come from the pK<sub>a</sub> values of NH, which are 2.1 and 5.4 (European Medicines Agency (EMA), 2009; US Food and Drug administration (FDA), 2007b) (dotted lines in Fig. 7). At pH values below 2.1 NH is diprotonated enabling a relatively high solubility. A relative large fraction of NH molecules in such an environment remain in solution, instead of being incorporated into Soluplus<sup>®</sup> micelles. This keeps the micelles small. In the pH region between 2.1 and 5.4, NH molecules are largely monoprotonated. It may be hypothesized that the NH molecules in such a state interact

very differently with the Soluplus<sup>®</sup> micelles. The NH may then in part be located in the outer, more hydrophilic ranges of the micelles but still need solubilisation for the non-protonated part of the molecule. This may in turn change the overall size of the micelles. At pH levels above 5.4, NH is largely unprotonated. Without solubilisation the NH molecules will precipitate from the dissolution medium. In the presence of Soluplus<sup>®</sup> NH is incorporated into the micelles. To test this hypothesis, spectroscopic studies should be performed in the future to localize NH in the micelles.

The size of the resulting micelles is also strongly dependent on the equivalent parts of Soluplus<sup>®</sup> that are present, as this determines the initial number of micelles over which the NH molecules can divide. The chloride counter-ion from NH may also have an impact on the micelle size through its influence on the ionic strength of the solution (Shi et al., 2016).

The clinical relevance of this phenomenon is still unclear as the micelles seem to minimize to their stomach size at pH > 6. Therefore, the formulation should be studied *in vivo*.

Various other parameters also influence micelle size, *i.e.* drug molecular size, partition coefficient and the presence of lipids and bile salts. In certain combinations with pK<sub>a</sub>'s of around 2 and 6–8 may cause other drugs to behave similarly.

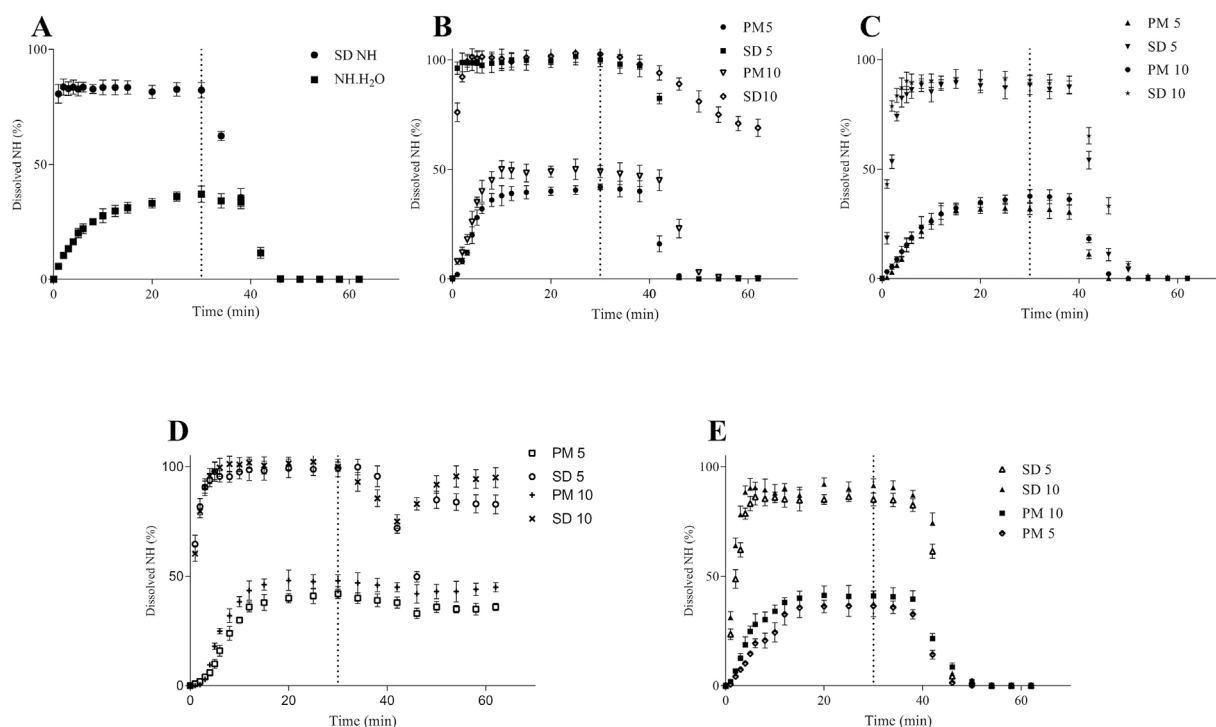
The dissolution and micelle size results from this study highlight unexplored possible characteristics of Soluplus<sup>®</sup>-containing formulations. Previous studies with spray-dried Soluplus<sup>®</sup> formulations did not employ pH-switches during dissolution and thus make no mention of micelle size changes (Ha et al., 2014;

Table 2

Components, weight ratios, and preparation methods of NH formulations.

Formulation	Components	Weight ratio (w/w)	Formulation method
A	Crystalline NH monohydrate	1/0	Pure drug
B	Amorphous NH	1/0	Spray drying
C	Crystalline nilotinib <sup>a</sup> , Kollidon VA64	1/5	Physical mixing
D	Crystalline nilotinib <sup>a</sup> , Kollidon VA64	1/5	Spray drying
E	Crystalline nilotinib <sup>a</sup> , Kollidon 12PF	1/5	Physical mixing
F	Crystalline nilotinib <sup>a</sup> , Kollidon 12PF	1/5	Spray drying
G	Crystalline nilotinib <sup>a</sup> , Soluplus <sup>®</sup>	1/5	Physical mixing
H	Crystalline nilotinib <sup>a</sup> , Soluplus <sup>®</sup>	1/5	Spray drying
I	Crystalline nilotinib <sup>a</sup> , Lutrol F68	1/5	Physical mixing
J	Crystalline nilotinib <sup>a</sup> , Lutrol F68	1/5	Spray drying
K	Crystalline nilotinib <sup>a</sup> , Kollidon VA64	1/10	Physical mixing
L	Crystalline nilotinib <sup>a</sup> , Kollidon VA64	1/10	Spray drying
M	Crystalline nilotinib <sup>a</sup> , Kollidon 12PF	1/10	Physical mixing
N	Crystalline nilotinib <sup>a</sup> , Kollidon 12PF	1/10	Spray drying
O	Crystalline nilotinib <sup>a</sup> , Soluplus <sup>®</sup>	1/10	Physical mixing
P	Crystalline nilotinib <sup>a</sup> , Soluplus <sup>®</sup>	1/10	Spray drying
Q	Crystalline nilotinib <sup>a</sup> , Lutrol F68	1/10	Physical mixing
R	Crystalline nilotinib <sup>a</sup> , Lutrol F68	1/10	Spray drying

<sup>a</sup> as hydrochloride monohydrate.



**Fig. 5.** A. Dissolution curve of crystalline NH monohydrate and spray dried NH. Dissolution curves of the physical mixtures and spray dried formulations with B. Kollidon VA64; C. Kollidon 12PF; D. Soluplus<sup>®</sup>; E. Lutrol 68F. The dotted line indicates the start of the pH-switch.

Lavra et al., 2017). The results presented here indicate that the application of a pH-switch may prove useful in uncovering possible unexpected dissolution behaviour of new formulations.

### 3.4. Electron microscopy (EM)

Fig. 8A and B presents the SEM micrographs of NH·H<sub>2</sub>O bulk powder and formulation V, respectively. Fig. 8A clearly shows the presence of large crystalline particles in the bulk powder. Additionally, Fig. 8B shows that the spray-dried formulation consists of smaller particles than the bulk powder, which likely plays an important role in the improved dissolution performance of formulation V.

To study the *in vitro* assembled micelles during the dissolution of the Soluplus<sup>®</sup> containing formulations, TEM was performed. Fig. 7C and D shows a micrograph of NH/Soluplus<sup>®</sup> micelles of formulation in SGF<sub>sp</sub> and SIF<sub>sp</sub>, respectively. The micelles have maintained their integrity, during the transition from SGF<sub>sp</sub> to SIF<sub>sp</sub>. Fig. 7C and D also shows that the size in SGF<sub>sp</sub> and SIF<sub>sp</sub> are similar. The micelles in the pH region 3–5 could not be successfully be visualized in this TEM set-up. The size of the micelles changed after addition of the phosphotungstic acid, likely due to the limited buffer capacity in this pH-region.

### 3.5. Fourier transform infrared spectroscopy

Crystalline NH monohydrate, amorphous NH and the spray dried formulations S through W (Table 3) with Soluplus<sup>®</sup> were physically examined using FTIR (Fig. 8C). The molecular structure of nilotinib contains heterocyclic systems with a trifluoromethyl moiety that interconnect through amine bridges resulting in characteristic absorption bands. The spectrum of formulation S (1:1 ratio) did not show any peak changes nor did it show any appearance or disappearance of characteristic peaks. This suggests that NH and Soluplus<sup>®</sup> do not suffer from detrimental intermolecular forces. The spray drying process removed the water of

crystallization and produced anhydrous amorphous NH. This is evident from the FTIR spectra which lack signals corresponding to water at around 2000 cm<sup>-1</sup> and 3200 cm<sup>-1</sup>. Karl Fischer titration results are consistent with these results and show <0.3% water content initially.

### 3.6. Modulated differential scanning calorimetry (MDSC)

MDSC was used to analyse the solid state characteristics of NH, Soluplus<sup>®</sup> and the formulations S to W.

The MDSC thermogram of crystalline NH monohydrate in Fig. 8D shows two clear endothermic events at 133 °C and 201 °C. The first indicates the loss of water of crystallization and the transition to the anhydrate form. This conversion to the anhydrate before melting is described in a patent text (Manley et al., 2005). The latter event corresponds to the melting point observed during analysis in the melting apparatus. As a comparison, Fig. 8D also shows a thermogram of crystalline NH anhydrate where the water of crystallization peak is not present. The MDSC spectrum in Fig. 8E of spray dried NH shows a glass transition temperature (T<sub>g</sub>) at 146 °C and no other thermal events up to degradation at 230 °C. This supports the observations from the FTIR experiments. Pure and spray dried Soluplus<sup>®</sup> have a T<sub>g</sub> as the only thermal event at 68 °C that corresponds to the 70 °C reported by BASF (Kolter et al., 2012). The spray dried formulations all show a single T<sub>g</sub> and no melting event. This indicates that NH is molecularly dispersed in

**Table 3**  
Weight ratios and T<sub>g</sub>'s of spray dried soluplus<sup>®</sup>-NH formulations.

Formulation	NH monohydrate: Soluplus <sup>®</sup>	T <sub>g</sub> (°C)
S	1: 1	95.3
T	1: 3	80.5
U	1: 5	75.9
V	1: 7	74.2
W	1: 10	73.7

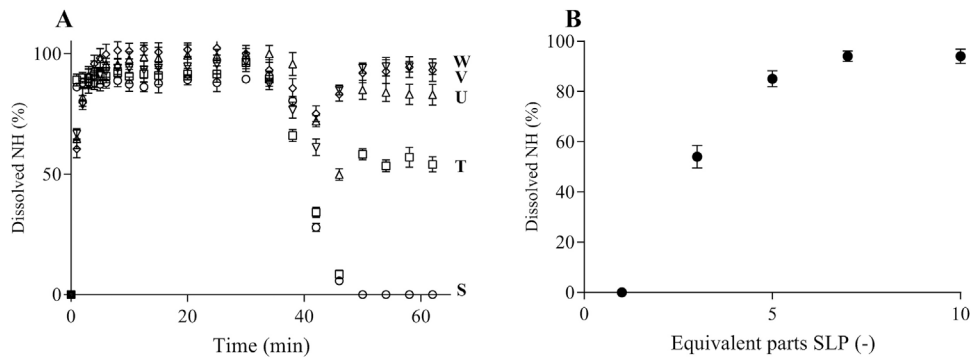


**Fig. 6.** Dissolution results of NH:Soluplus<sup>®</sup> formulations: A. Dissolution curves of NH:Soluplus<sup>®</sup> SDs with 5 compositions: S, T, U, V and W; B. Dissolved NH at pH 6.8 as a function of the Soluplus<sup>®</sup> equivalent parts.

the spray dried formulations. The trend in  $T_g$ 's is in line with the compositions of the formulations as described by formula 1 and listed in Table 3. These results aid in the conclusion that NH is molecularly dispersed through the matrix of Soluplus<sup>®</sup>.

$$\frac{1}{T_g} = \frac{w_1}{T_{g1}} + \frac{w_2}{T_{g2}} \quad (1)$$

Where  $w_x$  = weight fraction of component x and  $T_{gx}$  = glass transition temperature of component x.

### 3.7. Powder X-ray diffraction

XRD patterns were recorded to establish the solid state of the prepared spray dried dispersions. Fig. 8F shows the XRD patterns for crystalline NH monohydrate, NH:Soluplus<sup>®</sup> physical mixture (1:7) and spray dried NH and formulation V. The XRD pattern of crystalline NH monohydrate shows the characteristic sharp reflection peaks of crystallinity which have completely disappeared in the pattern of spray dried NH. The peaks of crystalline

material are also present in the physical mixtures of NH monohydrate and Soluplus<sup>®</sup>. The XRD patterns of the spray dried formulations lacked the sharp peaks as well. From the results of the physical characterization experiments it can be concluded that the raw NH monohydrate is crystalline and that it amorphicizes through the process of spray-drying and that the prepared solid dispersion also contains amorphous NH. This corresponds with the findings during the MDSC experiments, where no melting event was observed and only a single  $T_g$  was recorded for the formulations S to W.

### 3.8. Stability

Quality control testing of the 1:7 Soluplus<sup>®</sup> formulation showed near-complete dissolution in both USP SIF<sub>sp</sub> and SGF<sub>sp</sub>. SIF<sub>sp</sub> was chosen for stability tests because a decline in any of the formulations functional parameters (amorphicity, purity, etc.) is most likely to be noticed first in this medium because of the low intrinsic solubility of NH at SIF<sub>sp</sub> pH. During 6 months of storage in

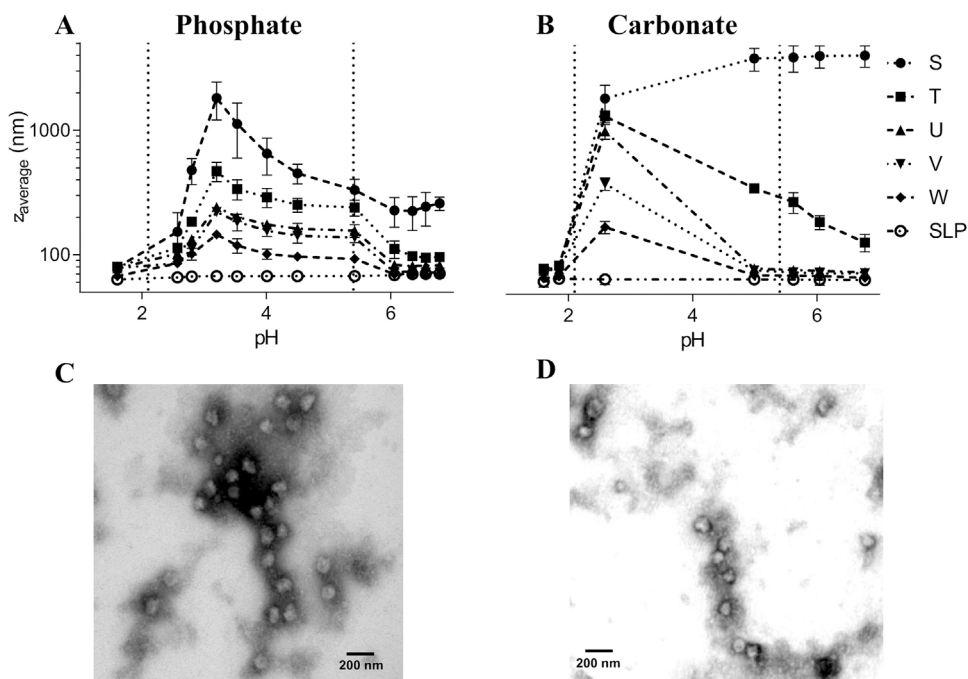


**Fig. 7.** Micelle diameters as a function of the pH of the dissolution medium: A. Phosphate SIF<sub>sp</sub>; B. Carbonate SIF<sub>sp</sub>. C. TEM micrograph of a representative NH:Soluplus<sup>®</sup> micelle in SGF<sub>sp</sub> (Magnification: 120000 $\times$ , high voltage: 100 kV); D. TEM micrograph of NH:Soluplus<sup>®</sup> micelles in SIF<sub>sp</sub> (Magnification: 120000 $\times$ , high voltage: 100 kV).

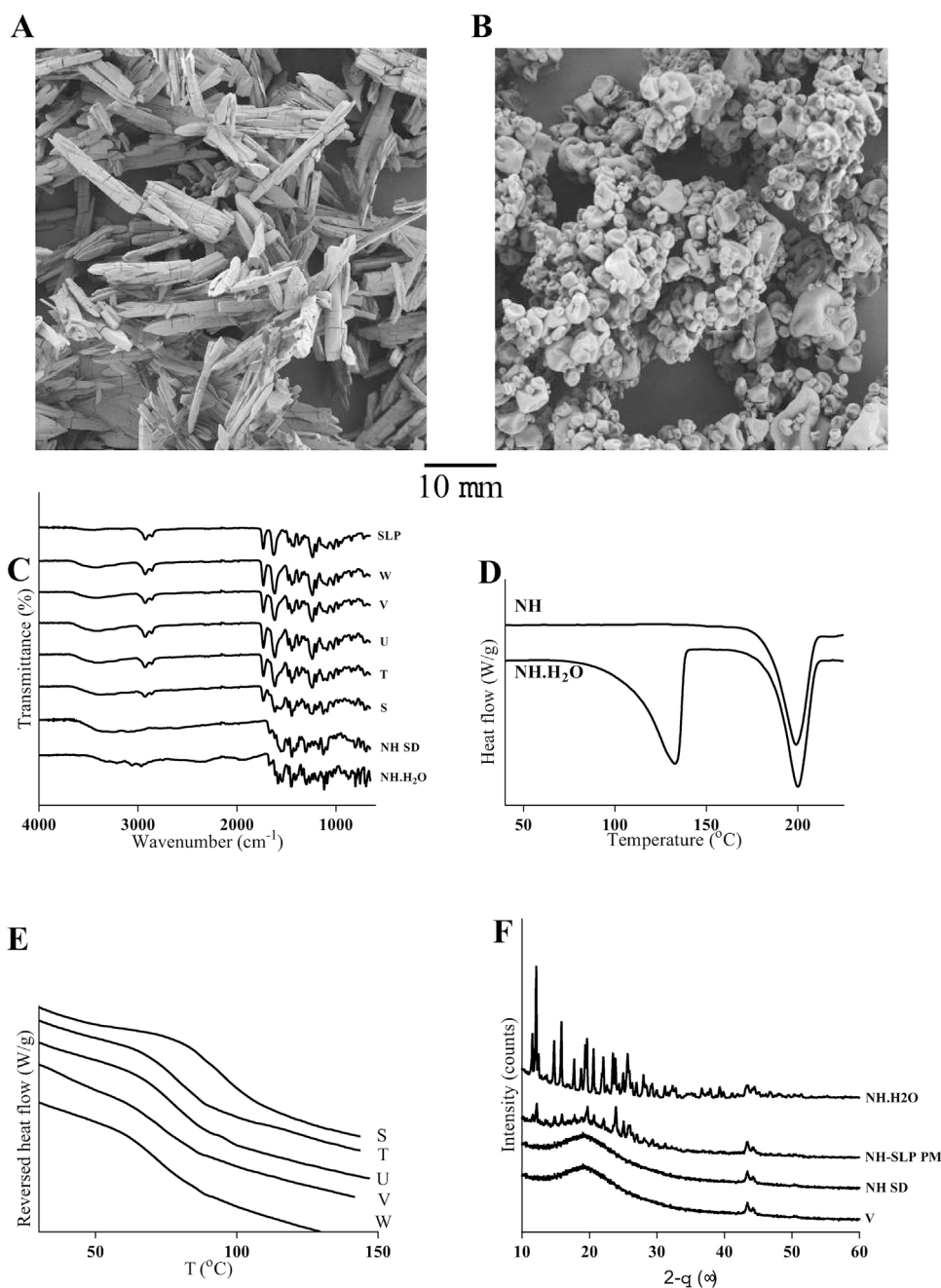


**Fig. 8.** Physicochemical characterization of NH (monohydrate) and formulations: A. SEM micrograph of NH·H<sub>2</sub>O bulk powder (Magnification: 500×, extra high tension: 2.00 kV); B. SEM micrograph of formulation V (Magnification: 500×, extra high tension: 2.00 kV); C. FTIR spectra of NH monohydrate, NH SD, formulations S, T, U, V and W and Soluplus<sup>®</sup>; D. DSC results of NH and NH monohydrate; E. MDSC results of NH:Soluplus<sup>®</sup> SD formulations S, T, U, V and W; F. XRD patterns of NH monohydrate, NH:Soluplus<sup>®</sup> physical mixture 1:7, NH SD and NH:Soluplus<sup>®</sup> formulation V, the peaks around 43° 2-θ originate from the sample holder.

**Table 4**  
Stability results of NH: Soluplus<sup>®</sup> (1:7) spray dried powder.

	Initial	6 months at 20–25 °C/60% RH, dark, open container	1 month at 40 °C/75% RH, dark, open container
Nilotinib peak purity (%)	100	99.6	99.7
Nilotinib dissolved at t = 45 min (%) <sup>a</sup>	95.2 (3.7)	94.0 (5.6)	94.1 (3.2)
Nilotinib dissolved at t = 120 min (%) <sup>a,b</sup>	94.9 (4.1)	93.8 (3.1)	94.0 (6.8)
Nilotinib dissolved at t = 240 min (%) <sup>a,b</sup>	94.6 (2.4)	93.9 (4.0)	93.5 (5.7)
XRD spectrum	Fully amorphous	Fully amorphous	Fully amorphous
Moisture (%) w/w	0.28	0.77	0.54

<sup>a</sup> Values are means and coefficients of variation.

<sup>b</sup> Time points were included to detect possible recrystallization of nilotinib HCl from the solution.

open containers at 20–25 °C and 60% relative humidity (RH) and after 1 month in open containers at 40 °C and 75% RH the formulation was subjected again to dissolution and assay tests (Table 4). In this period, no significant changes occurred in chemical or physical properties of the formulation. The moisture content did show an increase, this did not prove detrimental to the performance of the formulation. This indicative stability study should be extended in the future to map a conclusive stability profile of the formulation.

#### 4. Conclusion

This study shows that spray dried solid dispersions of NH are very effective in improving the low solubility of the NH in SGF<sub>sp</sub> and SIF<sub>sp</sub> compared to the marketed Tasigna<sup>®</sup> formulation. SDs containing Kollidon VA64 and Soluplus<sup>®</sup> were also effective in maintaining an increased solubility after the simulated pH switch from SGF<sub>sp</sub> to SIF<sub>sp</sub>. Of the polymer excipients tested, Soluplus<sup>®</sup> exhibited the best performance. The ratio 1:7 (NH:Soluplus<sup>®</sup>) was the lowest ratio that showed the highest performance and was thus developed further. Stability of the latter formulation was established for at least 6 months. This study further presents characteristic micelle behaviour of the NH:Soluplus<sup>®</sup> combinations when exposed to aqueous environments at different pH levels that may be relevant for other compounds in combination with Soluplus<sup>®</sup>. Hence, Soluplus<sup>®</sup> in a ratio of 7:1 with NH demonstrates a great increase in solubility of NH. Whether this leads to a higher bioavailability and a possibly reduced variability needs to be tested *in vivo*. Although a 1:7 ratio would make for a bulky tablet or capsule, the increase in bioavailability might enable smaller doses to be administered which could reduce the final formulation size.

#### Acknowledgements

The authors wish to thank C. Brouwer and G.A. Jacob for their valuable contribution to execution of the experiments.

#### References

- Andersson, P., VonEuler, M., Beckert, M., 2014. Comparable pharmacokinetics of 85 mg RightSize nilotinib (XS003) and 150 mg Tasigna in healthy volunteers using a hybrid nanoparticle-based formulation platform for protein kinase inhibitors. ASCO Annual Meeting (2014).
- Bansal, S.S., Kaushal, A.M., Bansal, A.K., 2007. Molecular and thermodynamic aspects of solubility advantage from solid dispersions. *Mol. Pharm.* 4, 794–802.
- Chiu, W.L., Riegelman, S., 1971. Pharmaceutical applications of solid dispersion systems. *J. Pharm. Sci.* 60, 1281–1302.
- Colombo, S., Brisander, M., Haglöf, J., Sjövall, P., Andersson, P., Østergaard, J., Malmsten, M., 2015. Matrix effects in nilotinib formulations with pH-responsive polymer produced by carbon dioxide-mediated precipitation. *Int. J. Pharm.* 494, 205–217.
- European Medicines Agency (EMA), 2007. European Public Assessment Report Tasigna.
- European Medicines Agency (EMA), 2009. Assessment Report Tasigna. EPAR.
- Einfalt, T., Planinsek, O., Hrovat, K., 2013. Methods of amorphization and investigation of the amorphous state. *Acta Pharm.* 63, 305–334.
- US Food and Drug Administration (FDA), 2007a. Clinical Pharmacology and Biopharmaceutics Review Tasigna.
- US Food and Drug Administration (FDA), 2007b. Chemistry Review Tasigna.
- US Food and Drug Administration (FDA), 2010. Prescribing Information Tasigna(R).
- Ha, E.-S., Baek, I., Cho, W., Hwang, S.-J., Kim, M.-S., 2014. Preparation and evaluation of solid dispersion of atorvastatin calcium with Soluplus<sup>®</sup> by spray drying technique. *Chem. Pharm. Bull. (Tokyo)* 62, 545–551.
- Herbrink, M., Nuijten, B., Schellens, J.H.M., Beijnen, J.H., 2015. Variability in bioavailability of small molecular tyrosine kinase inhibitors. *Cancer Treat. Rev.* 41, 412–422.
- Janssens, S., Van den Mooter, G., 2009. Review: physical chemistry of solid dispersions. *J. Pharm. Pharmacol.* 61, 1571–1586.
- Jesson, G., Brisander, M., Andersson, P., Demirbükler, M., Derand, H., Lennernäs, H., Malmsten, M., 2014. Carbon dioxide-mediated generation of hybrid nanoparticles for improved bioavailability of protein kinase inhibitors. *Pharm. Res.* 31, 694–705.
- Kawabata, Y., Wada, K., Nakatani, M., Yamada, S., Onoue, S., 2011. Formulation design for poorly water-soluble drugs based on biopharmaceutics classification system: basic approaches and practical applications. *Int. J. Pharm.* 420, 1–10.
- Keen, J.M., McGinity, J.W., Williams, R.O., 2013. Enhancing bioavailability through thermal processing. *Int. J. Pharm.* 450, 185–196.
- Kolter, K., Karl, M., Gryczke, A., 2012. Hot-Melt Extrusion with BASF Pharma Polymers, 2nd ed. BASF SE, Ludwigshafen.
- Lavra, Z.M.M., Pereira de Santana, D., Ré, M.I., 2017. Solubility and dissolution performances of spray-dried solid dispersion of Efavirenz in Soluplus. *Drug Dev. Ind. Pharm.* 43, 42–54.
- Li, Y.-C., Rissanen, S., Stepniowski, M., Cramariuc, O., Róg, T., Mirza, S., Xhaard, H., Wyrwal, M., Kepczynski, M., Bunker, A., 2012. Study of interaction between PEG carrier and three relevant drug molecules: piroxicam, paclitaxel, and hematoporphyrin. *J. Phys. Chem. B* 116, 7334–7341.
- Lohani, S., Cooper, H., Jin, X., Nissley, B.P., Manser, K., Rakes, L.H., Cummings, J.J., Fauty, S.E., Bak, A., 2014. Physicochemical properties, form, and formulation selection strategy for a biopharmaceutical classification system class II preclinical drug candidate. *J. Pharm. Sci.* 103, 3007–3021.
- Manley, P.W., Shieh, W.-C., Sutton, P.A., Karpinski, P.H., 2005. Crystalline Forms of 4-methyl-n-[3-(4-methyl-imidazol-1-yl)-5-trifluoromethyl-phenyl]-3-(4-pyridin-3-yl-pyrimidin-2-ylamino)-benzamide. (WO2007015870A2).
- Mudie, D.M., Amidon, G.L., Amidon, G.E., 2010. Physiological parameters for oral delivery and *in vitro* testing. *Mol. Pharm.* 7, 1388–1405. doi:http://dx.doi.org/10.1021/mp100149j.
- Newman, A., Knipp, G., Zografi, G., 2012. Assessing the performance of amorphous solid dispersions. *J. Pharm. Sci.* 101, 1355–1377.
- Rahman, M.A., Harwansh, R., Mirza, M.A., Hussain, S., Hussain, A., 2011. Oral lipid based drug delivery system (LBDDS): formulation, characterization and application: a review. *Curr. Drug Deliv.* 8, 330–345.
- Savjani, K.T., Gajjar, A.K., Savjani, J.K., 2012. Drug solubility: importance and enhancement techniques. *ISRN Pharm.* 2012, 1–10.
- Shi, N.-Q., Lai, H.-W., Zhang, Y., Feng, B., Xiao, X., Zhang, H.-M., Li, Z.-Q., Qi, X.-R., 2016. On the inherent properties of Soluplus and its application in ibuprofen solid dispersions generated by microwave-quench cooling technology. *Pharm. Dev. Technol.* 1–14.
- Shukla, S., Skoumbourdis, A.P., Walsh, M.J., Hartz, A.M.S., Fung, K.L., Wu, C.-P., Gottesman, M.M., Bauer, B., Thomas, C.J., Ambudkar, S., 2011. Synthesis and characterization of a BODIPY conjugate of the BCR-ABL kinase inhibitor Tasigna (nilotinib): evidence for transport of Tasigna and its fluorescent derivative by ABC drug transporters. *Mol. Pharm.* 8, 1292–1302.
- Singh, B., Bandopadhyay, S., Kapil, R., Singh, R., Katara, O., 2009. Self-emulsifying drug delivery systems (SEDDS): formulation development, characterization, and applications. *Crit. Rev. Ther. Drug Carrier Syst.* 26, 427–521.
- Tanaka, C., Yin, O.Q.P., Sethuraman, V., Smith, T., Wang, X., Grouss, K., Kantarjian, H., Giles, F., Ottmann, O.G., Galitz, L., Schran, H., 2010. Clinical pharmacokinetics of the BCR-ABL tyrosine kinase inhibitor nilotinib. *Clin. Pharmacol. Ther.* 87, 197–203. doi:http://dx.doi.org/10.1038/clpt.2009.208.
- Viel, Q., Brandel, C., Cartigny, Y., Eusébio, M.E.S., Canotilho, J., Dupray, V., Dargent, E., Coquerel, G., Petit, S., 2017. Crystallization from the amorphous state of a pharmaceutical compound: impact of chirality and chemical purity. *Cryst. Growth Des.* 17, 337–346.
- Yu, L., 2001. Amorphous pharmaceutical solids: preparation, characterization and stabilization. *Adv. Drug Deliv. Rev.* 48, 27–42.